Polymer Bulletin 48, 199–206 (2002)

Polymer Bulletin

Inhibition of crystalline structure development in a reactive polycarbonate-poly(butyleneterephthalate) blend

Arthur N. Wilkinson (✉)[1], Steven B. Tattum[1], Anthony J. Ryan[2]

[1]Department of Chemistry & Materials, Manchester Metropolitan University, John Dalton Building, Manchester M1 5GD, United Kingdom
[2]Department of Chemistry, University of Sheffield, Dainton Building, Brook Hill, Sheffield S3 7HF, United Kingdom

Received: 17 September 2001/Revised version: 21 February 2002/ Accepted: 25 February 2002

Summary

The crystallization behaviour of PBT and a reactive 50/50 PBT-PC blend were studied using synchrotron SAXS/DSC and TEM. The scattering data showed PBT crystallization to be inhibited in the blend due to PBT-PC transesterification, resulting in a progressive reduction in both melting and recrystallization temperatures and the degree of crystallinity developed. Analysis of the SAXS data using a one-dimensional correlation function showed PBT to exhibit an ordered lamellar morphology, whereas in the blend stacking of lamellae appeared to be inhibited. TEM of PBT-PC blends confirmed that PBT lamellae were randomly-oriented.

Introduction

Blends of polycarbonate (PC) and poly(butylene terephthalate) (PBT) [1-10] exhibit complex melt behaviour, in which transesterification reactions between the homopolymers, liquid-liquid phase separation and crystallization of the PBT may occur. A 50:50 PC-PBT blend studied using time-resolved light scattering has been shown [6] to exhibit lower critical solution temperature (LCST) type phase behaviour with a spinodal temperature (T_S) of 198 °C. Thus, once a PC-PBT blend cools below T_S it will begin to phase mix and form a homogeneous mixture. However, phase dissolution, which is not a rapid process [11, 12], is in kinetic competition with crystallization of the PBT which will initiate at temperatures below T_m (~220 °C). PBT exhibits rapid crystallization and, despite some retardation due to the presence of phase-mixed PC, crystallization of the PBT-rich phase is still relatively rapid in most PC-PBT blends [8,9]. Consequently, structure development within these materials tends to be dominated by PBT crystallization, which prevents significant phase dissolution and 'locks in' the biphasic morphology developed during melt blending [3-5, 7, 8, 10]. However, the propensity of PBT to crystallize is reduced via extensive transesterification, until eventually the blend is transformed into an amorphous, homogeneous mixture comprising homopolymers and various AB-type copolymers. A previous paper [9] from this study [7,9,10] described the changes in SAXS/WAXS intensities during thermal cycling of a reactive PC-PBT blend. This paper presents additional results on the

inhibition of crystallization of PBT during thermal cycling of this PC-PBT blend, via an analysis of the SAXS data using a one-dimensional correlation function in terms of an ideal lamellar morphology.

Experimental

A 50:50 w/w blend of PC (Makrolon 2405, ex. Bayer) and PBT (Pocan B1505, ex. Bayer) was prepared by melt blending in a Brabender PL2000 Plasticorder. Rotor speed, mixing time, chamber temperature and fill ratio were maintained, respectively, at 75 rpm, 2 minutes, 230°C and 0.8. Transesterification was promoted using an alkyl titanium catalyst (tetrakis(2-ethyl-hexyl)titanate, Tyzor TOT, ex. Du Pont), at a level calculated to give 200 ppm titanium in the blend. Organic titanates are efficient catalysts for melt transesterification between PC and PBT [2,7]. Simultaneous SAXS/WAXS/DSC measurements were made on beamline 8.2 of the SRS at the CLRC Daresbury laboratory, the experimental set-up for which has been described in detail elsewhere [13]. Specimens were prepared for SAXS/WAXS by encapsulating a thin slice of material (≈ 0.5 mm thick) in a DSC pan fitted with mica windows. These pans were cycled in a Linkam DSC [14] at 20 °C min^{-1} between 30 and 250 °C, with a one-minute hold period at the maximum and minimum temperatures. WAXS data were reported previously [9]. Transmission electron microscopy was conducted using a Philips EM400 , at an accelerating voltage of 100 keV. Samples for TEM were prepared using a Reichert Ultracut microtome fitted with a Drukker diamond knife. Specimens were stained by exposure to RuO_4 vapours for 3 hours .

Results and discussion

SAXS data are shown in Figure 1 for pure PBT and the blend after the same thermal history. The plots of Lorentz-corrected intensity versus scattering vector show the SAXS profile for the blend to exhibit a lower intensity maxima (designated q^*) at a lower value of q. In addition, the scattering peak for the blend is much broader ($\Delta q/q^* \approx 2$, Δq = peak width at half-maximum peak height) and more shallow than the peak for PBT ($\Delta q/q^* \approx 1.5$). Interdomain spacings (d) were calculated from the scattering maxima using Bragg's law ($d=2\pi/q^*$) to give long spacing values of d (PBT) ≈ 160 Å and d (blend) ≈ 210 Å. This grade of PBT has been observed to exhibit reproducible SAXS/WAXS crystallization/melting data during repeated thermal cycling [9]. However, the differences between the SAXS profiles shown in Figure 1 were observed to increase during thermal cycling as PBT crystallization was inhibited in the blend by PC-PBT transesterification [9].

The scattered intensity from SAXS can be related to the degree of crystallization via the relative invariant, Q', which is linear in the electron density difference $\langle\eta^2\rangle$ between the crystalline and amorphous phases and quadratic in the volume fraction of crystals ϕ, giving $Q' = \phi(1-\phi)\langle\eta^2\rangle$. Values of Q' were calculated via Simpson's rule integration of the curves of $I(q, t)q^2$ versus q between the experimental limits of the first and last reliable data points (i.e. from q = 0.01 to 0.18 $Å^{-1}$). Plots of Q' versus temperature for the PBT and the blend are shown in Figure 2(a) and (b), respectively. The Q' data for the PBT (Figure 2(a)) shows the good reproducibility in melting and recrystallization behaviour over four thermal cycles. The initial melting behaviour of

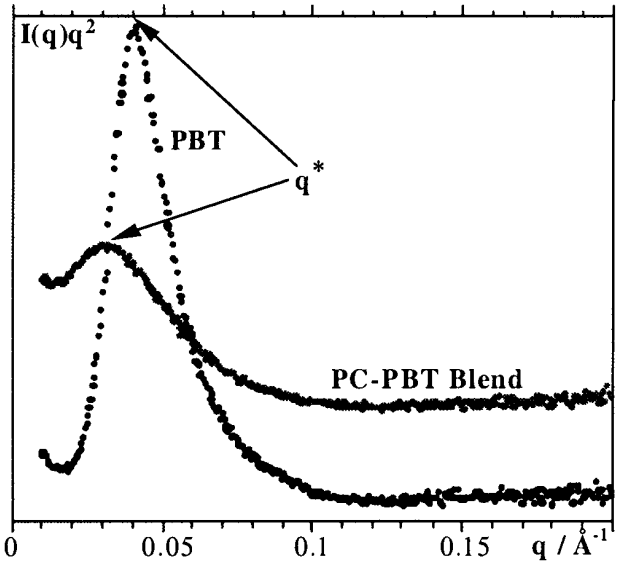

Figure 1. Lorentz-corrected intensity vs. scattering vector for the PBT and the 50:50 PBT/PC blend at the same temperature (160˚C) during the second heating cycle.

the as-received PBT (cycle 1) reflects its different thermal history, but during all four cycles the PBT exhibits a rapid decrease in Q' due to melting at $T_m \approx 220$ ˚C, and a corresponding increase in Q' at $T_c \approx 200$ ˚C as recrystallization occurs. The glass transition of the PBT is also evident as a change in slope of the invariant curves at $T_g \approx 40$ ˚C due to the change in slope of the expansion coefficient of the amorphous phase c.f. the crystalline phase. The Q' data for the blend (Figure 2(b)) illustrates well the effects of transesterification. The initial heating cycle of the blend (cycle 1) shows melting at $T_m \approx 215$ ˚C, recrystallization at $T_c \approx 200$ ˚C and two glass transitions; a broad change in slope beginning at ≈ 60 ˚C attributed to a PBT-rich phase, and a higher temperature transition at ≈ 150 ˚C attributed to a PC-rich phase. However, over the next three cycles the blend exhibits only one discernible glass transition, which shifts from ≈ 60 ˚C to ≈ 90 ˚C as a result of transesterification. The latter value agrees well with the value of 86˚C calculated for a homogeneous 50/50 PC-PBT material using the Fox equation. Transesterification also has significant effects on melting and recrystallization behaviour. Thus, over the four thermal cycles the degree of crystallinity (indicated by the value of Q') is significantly reduced, and the values of T_m and T_c are seen to decrease by approximately 20 ˚C and 10 ˚C, respectively.

The reduction in degree of crystallinity of the PBT in the blend resulting from transesterification is also illustrated in Figure 3, in which Q' is shown as a function of time for an extended period of eight thermal cycles. Thus, during this extended thermal cycling the general level of Q', which relates to the degree of crystallisation, is seen to decrease continuously as transesterification proceeds.

The SAXS data were analysed using a 1-d correlation function in terms of an ideal lamellar morphology [15-17]. The correlation function, designated γ_1, is essentially a Fourier transform of a given 1-d SAXS curve, and is often interpreted in terms of an imaginary rod moving through the structure of the material from which the SAXS curve was obtained, so that $\gamma_1(r)$ may be considered as the probability that the rod is of length, *r*, with equal electron densities at either end. Hence, a frequently occurring

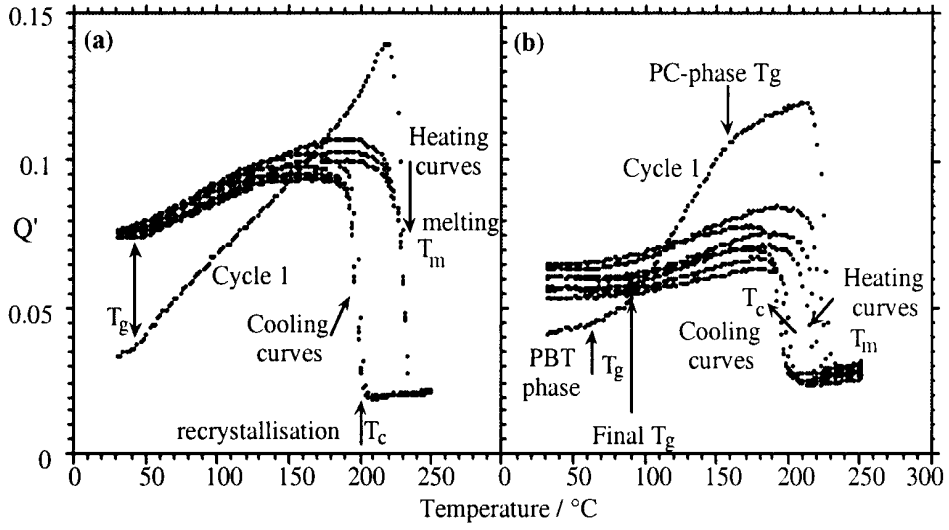

Figure 2. Temperature dependence of the SAXS invariant Q' for (a) PBT and (b) the 50:50 PBT/PC blend over four thermal cycles.

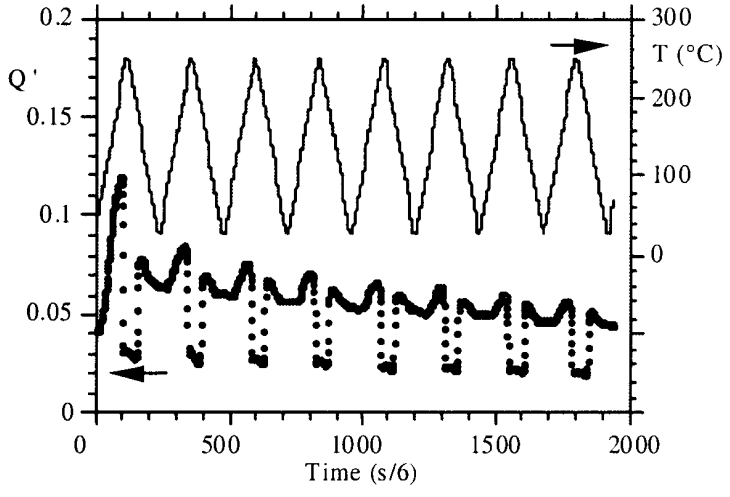

Figure 3. PBT/PC Blend: variations in invariant Q' during 8 thermal cycles, for which the temperature profile T(t) is shown.

spacing within a structure is manifested as a peak in $\gamma_1(r)$. To calculate $\gamma_1(r)$ [18], firstly the SAXS data were extrapolated to the limits of q = 0 and q = ∞, followed by Fourier transformation. Secondly, $\gamma_1(r)$ was interpreted on the basis of an ideal lamellar morphology [16] to yield the long spacing (d_γ), the lamellar thickness (L_γ) and the local degree of crystallinity (X_γ). Correlation functions ($\gamma_1(r)$ vs. r) are shown in Figure 4 for the PBT and the blend after the same thermal history (i.e. the SAXS curves of Fig. 1). For the PBT, the series of decaying peaks in $\gamma_1(r)$ is indicative of a

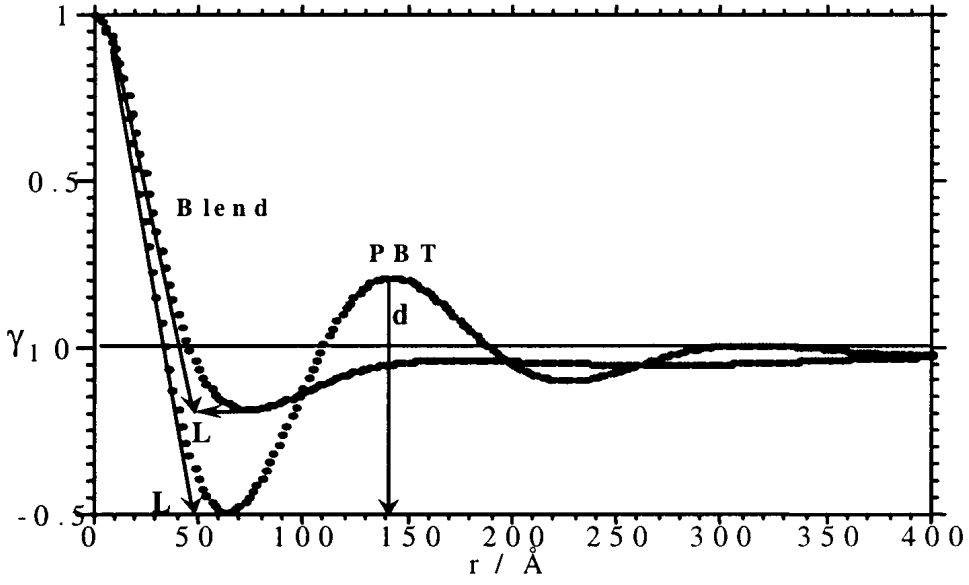

Figure 4. One-dimensional correlation functions for PBT and the 50:50 PBT/PC blend.

two-layer phase system, typical of a semi-crystalline thermoplastic [18], and both the most probable long spacing ($d_\gamma \approx 140$ Å) and the most probable lamellar thickness ($L_\gamma \approx 50$ Å) may be obtained as indicated in Fig. 4. The value of d_γ (≈ 140 Å) differs from that calculated using Bragg's Law and q^* (≈ 160 Å), the reason being that the $\gamma_1(r)$ value is based on an analysis of only that fraction of the sample exhibiting a regular lamellar morphology. The correlation function for the blend (Fig. 4) indicates that the morphology present is very different to that of the PBT. A value for the most probable lamellar thickness ($L_\gamma \approx 50$ Å) could be determined from $\gamma_1(r)$, but no discernible value of long spacing to compare with that calculated using Bragg's Law of $d \approx 210$ Å. The $\gamma_1(r)$ curve for the blend was observed to merely oscillate weakly, and finally reach $\gamma_1(r) = 0$ at ≈ 800Å. It must be concluded that even at this relatively early stage in the thermal history of the blend the morphology of the PBT component can no longer be interpreted in terms of an ordered lamellar model. The PBT morphology at this point is still lamellar, but is no longer ordered into discrete stacks.
Figure 5 shows a plot of morphological data for PBT, calculated using $\gamma_1(r)$, as a function of time during the initial four thermal cycles. As discussed previously, the first cycle reflects the thermal history of the as-received PBT. Over the cycles that follow, the PBT exhibits excellent reproducibility throughout the crystallization and melting processes. Thus, as the PBT is cooled from the hold temperature of 250°C the local degree of crystallinity (X_γ) is observed to increase sharply as crystallization commences. The most probable value of L_γ for the lamellae formed during initial recrystallization (i.e. at $T \approx T_c$) is ≈ 50 Å. At this point relatively few lamellae have formed and the spacing between domains of equal electron density is therefore relatively large, as is the spacing for the stack (d_γ = amorphous layer thickness + L_γ). However, as cooling continues progressively thinner lamellae are formed as the melt cools below T_c, and these fractionation processes reduce the most probable values for the four morphological parameters (i.e. the amorphous layer thickness, d_γ, L_γ and X_γ) as the melt temperature falls. When the temperature drops below the T_g of PBT

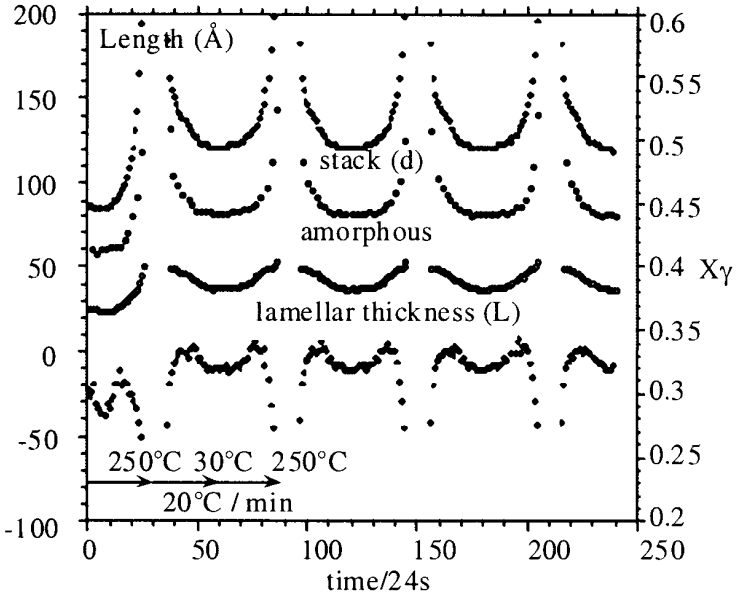

Figure 5. Morphological data for PBT derived from the correlation function (long spacing (d_γ), lamellar thickness (L_γ) local degree of crystallinity (X_γ)), as a function of time.

(≈ 40°C), vitrification effectively 'locks in' the morphology, and consequently the four parameters show no change. As the thermal cycle continues, and the temperature is raised above the T_g of PBT and towards T_m, the thinner lamellae melt first and the four morphological parameters show corresponding increases.
The crystalline morphologies of two PC-PBT blends of low degrees of transesterification are illustrated in the TEM micrographs of Figure 6, in which the PC appears as the darker phase.

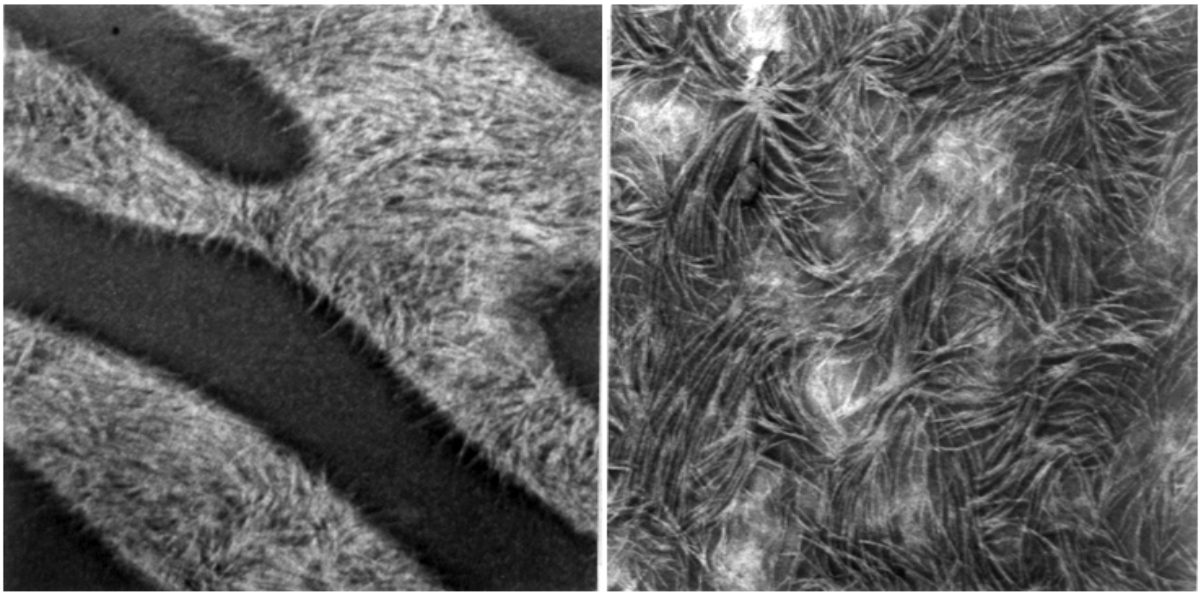

(a) **(b)**

Figure 6. TEM micrographs of blends stained with Ru O_4: **(a)** 25T (x33k), **(b)** 50T (x20k).

These lightly-catalysed 50/50 blends contain only 25 ppm (25T, Fig. 6a) or 50 ppm (50T, Fig. 6b) of Ti, compared to the 200 ppm (200T blend) used in the current study. FTIR analysis of these blends, using a technique described in [10], found no statistically significant evidence of transesterification, although low levels of transesterification are extremely difficult to quantify using IR spectroscopy [2, 10]. FTIR analysis of the 200T blend used in the present study revealed a degree of transesterification of ≈ 20% after two thermal cycles in a DSC [19], therefore it is reasonable to assume that the 25T and 50T blends have experienced a lower degree of transesterification than the 200T blend. However, despite the relatively low degrees of transesterification experienced by these blends, there is significant disruption of the spherulitic crystalline morphology typical of PBT. The 25T blend (Fig. 6a) exhibits a bicontinuous two-phase morphology of PC- and PBT-rich phases. However, the PBT lamellae appear randomly oriented with no evidence of spherulitic structure. In addition, the PBT lamellae are observed to penetrate into the PC phase, indicating that a level of PBT resides within the PC phase. Upon increasing the catalyst level to 50 ppm Ti, the two-phase morphology is displaced by an apparently continuous semi-crystalline phase. Figure 6b shows sheaf-like bundles of lamellae to have nucleated, grown and impinged to form a heavily entangled mass. Thus, the morphologies of both the 25T and 50T blends correlate well with the fact that only a relatively limited correlation function analysis was possible with the 200T blend in terms of an ordered lamellar morphology.

Conclusions

PBT formed well-ordered lamella stacks which exhibited reproducible melting and recrystallization behaviour. The advent of transesterification in a 50/50 PBT-PC blend caused the PBT lamellar structure to be disturbed, most likely due to PC contamination of the intralamellar amorphous regions. This was manifest as non-ideal lamellar crystals with random morphology.

Acknowledgements. The authors would like to thank Bayer and Du Pont for supplying materials and the EPSRC for providing SRS beamtime under grant GR/M22116.

References

1. Wahrmund DC, Paul DR, Barlow J, (1978) *J App Polym Sc*i 22 :2155
2. Devaux J, Godard P, Mercier JP, (1982), *Polym Eng & Sci*, 22:229.
3. Hobbs SY, Groshans VL, Dekkers MEJ, Shultz AR, (1987), *Poly Bull* 17:335.
4. Delimoy D, Bailly C, Devaux J, Legras R, (1988), *Polym Eng & Sci*, 28:104.
5. Dekkers MEJ, Hobbs SY, Bruker I, Watkins VH, (1990), *Polym Eng & Sci*, 30:1628
6. Okamoto M, Inoue T, (1994), *Polymer*, 35:257.
7. Wilkinson AN, Cole D, Tattum SB, (1995), *Polymer Bulletin*, 35:751.
8. Delimoy D, Goffaux B, Devaux J, Legras R, (1995), *Polymer*, 36:3255.
9. Wilkinson AN, Tattum SB, Ryan AJ, (1997), *Polymer*, 38: 1923.
10. Tattum SB, Cole D, Wilkinson AN, (2000), *J Macromol Sci Phys*, B39 (4):459.
11. Kumaki J, Hashimoto T, (1986), *Macromolecules*, 19:763.
12. Okamoto N, Shiomi K, Inoue T, (1995), *Polymer*, 36:87.
13. Bras W, Derbyshire G, Devine A, Clarke SM, Cooke J, Komanscheck BU, Ryan AJ, (1995), *J. Appl. Cryst*., 28:26.
14. Bras W, Derbyshire GE, Ryan AJ, Mant G, Felton A, Lewis RA, Hall CJ, Greaves GN,

(1993), *Nuclear Instruments and Methods in Physics Research*, A326:587.
15. Vonk CG, (1975), *J. Appl. Cryst.*, 8:340.
16. Strobl GR, Schnieder MJ, *J Polym Sci, Polym Phys Ed*, (1981), 19:1361.
17. Ruland W, (1971), *J Appl Cryst*, 4:70.
18. Ryan AJ, Stanford JL, Bras W, Nye TMW, (1997), *Polymer*, 38:759.
19. Tattum SB, (1997), PhD Thesis, Manchester Metropolitan University, UK.